BROAD GENERALIZATION OF THE VENTRILOQUISM AFTEREFFECT ACROSS SOUND FREQUENCIES

Rachel Ege*, Nina C. Haukes*, A. John van Opstal, Marc M. van Wanrooij

Radboud University, Donders Institute for Brain, Cognition and Behaviour, Donders Centre for Neuroscience, Nijmegen, The Netherlands

*Shared first authorship

E-mail: marc.vanwanrooij@donders.ru.nl

Abstract

Humans localise sounds in the horizontal plane by processing level and timing differences between the ears. This neurocomputational process is continuously and adaptively calibrated using visual input, as seen in the ventriloquism aftereffect — a shift in sound perception toward a previously seen light. It is unknown from where in the brain this aftereffect originates; adaptation could occur at an early level in the auditory system where neurons are narrowly tuned to frequency, at a later level in the auditory system where localisation cues are extracted, or outside the auditory system at a higher-level spatial map. To investigate this, we examined how the ventriloquism aftereffect generalizes across sound frequencies. Participants localised seven narrowband sounds (0.5–8 kHz), targeting different localisation cues. We found that sound localisation accuracy in darkness varied slightly with frequency. When sounds were paired with a visual stimulus that was offset by 10 deg, participants exhibited a pronounced bias toward the light – about ~63% – corresponding to the well-known ventriloquism effect. The bias was stronger for narrowband compared to broadband sounds. After exposure to a block of these audiovisual stimuli, a ventriloquism aftereffect in the form of a spatial bias of ~12% was observed across all tested frequencies, largely independent of the frequency of the exposure sound. These findings indicate that the aftereffect generalizes beyond the specific frequency used during adaptation, suggesting it may stem from adaptation within a multisensory motor map.

Keywords – Humans, Sound Localisation, Auditory Perception, Space Perception, Multisensory Integration, Adaptation

Introduction

Horizontal sound localisation relies on processing of binaural localisation cues[1,2]: interaural time differences (ITDs), which result from differences in sound arrival time between the ears and are prominent at low frequencies (≲1.5 kHz), and interaural level differences (ILDs), which arise from the acoustic shadow of the head and are prominent at higher frequencies (≳2–3 kHz). To maintain accurate auditory spatial perception, the mapping between these cues and external space must be continuously calibrated. Vision can serve as a calibration signal, which is illustrated by the ventriloquism aftereffect. After repeated exposure to a sound and a spatially displaced light, the perceived sound location remains biased toward the previous visual input—even in the absence of the light[3–6]. The ventriloquism aftereffect has been widely documented[7–18], yet it remains unclear how this effect generalizes. Specifically, it is unknown whether the aftereffect generalizes across different frequencies, across binaural localisation cues (ITDs and ILDs), or across a higher-order spatial representation. Examining how the ventriloquism aftereffect behaves across spectral conditions can help distinguish between these possibilities. In this study, we assess how the spectral content of sounds influences the strength and generalization of the aftereffect.

Previous research[4–6,9,13] suggests that the ventriloquism aftereffect could originate from different levels of auditory processing, leading to three competing hypotheses (schematically illustrated in Fig. 1): (i) the frequency hypothesis, (ii) the cue hypothesis, and (iii) the space map hypothesis. The three mechanisms describe different levels in auditory processing. First, the frequency hypothesis (Fig. 1a) states that the audiovisual interactions between the sound and the light take place at a level where the auditory input is tonotopically represented. If the audiovisual interactions take place at this level, the ventriloquism aftereffect is expected to only occur for sound frequencies that lie within the critical spectral band around the exposure frequency[19,20]. This would mean there will be no generalization of the aftereffect to other sound frequencies (support for this hypothesis[4,5,13]).

Second, the cue hypothesis (Fig. 1b) states that the audiovisual interactions take place at a stage in auditory processing where the binaural spatial cues have been extracted. Broadband sounds, containing a wide range of frequencies, can be localised using both cues, whereas sounds with only frequencies between 1.5 and 3 kHz provide weak or ambiguous localisation cues. By using narrowband sounds with different frequencies, we can target different localisation cues (low frequency ITDs, high frequency ILDs). If the cue hypothesis holds, the ventriloquism aftereffect will generalize among all sound frequencies that share the same localisation cue as the exposure sound, but not to sound frequencies that rely on the other localisation cue (to our knowledge, the only study that directly tested this prediction found no evidence in support of it [9]).

Third, the space map hypothesis states that audiovisual interactions occur at a multisensory or motor stage where auditory cues have been integrated with non-auditory cues, for example at an eye-centred motor map[2,12,21] (Fig. 1c). If this holds, the ventriloquism aftereffect will generalize across all sounds (support for this hypothesis[6,9]).

Alternatively, the degree of generalization may not depend on the stage of auditory processing, but rather on how auditory neurons across the auditory system are tuned to frequency as a function of sound intensity[22,23]. At high sound intensities, auditory neurons tend to respond to a broad range of frequencies, whereas at lower intensities, their frequency tuning becomes narrower. If this intensity hypothesis holds, the ventriloquism aftereffect should generalize fully across frequencies only for high sound levels (exceeding 66 dB according to simulations[23]). At lower intensities, the aftereffect is expected to be limited or absent due to more selective frequency tuning. This account could reconcile discrepancies between existing studies supporting frequency-specific (tonotopy) versus frequency-general (space map) hypotheses.

In this study, we used an absolute pointing task based on head movements to quantify how participants localised sounds across three experimental phases, conducted over three separate sessions. Each session featured a different exposure sound—either a low-frequency, high-frequency, or broadband sound—paired with a spatially displaced visual stimulus. In the pre-exposure phase, we assessed baseline localisation accuracy for eight sounds (one broadband and seven narrowband) presented in isolation, without any visual stimulus. In the exposure phase, we measured the immediate ventriloquism effect—a shift in perceived sound location caused by a visual stimulus offset by 10°—for the session-specific exposure sound. Finally, in the post-exposure phase, we assessed the ventriloquism aftereffect by measuring localisation responses to all eight sounds again, now without any visual input. This design allowed us to test whether exposure to a single sound leads to a lasting recalibration of sound localisation that generalizes across frequencies. All sounds were presented at a relatively low intensity (55 dB). This is a sound level at which Magosso et al. [23] predict minimal or no generalization of the aftereffect, based on prior findings[4,5] of limited generalization at low intensities (45 and 60 dB), in contrast to studies at higher intensities (66 and 70 dB) that report generalization[6,9].

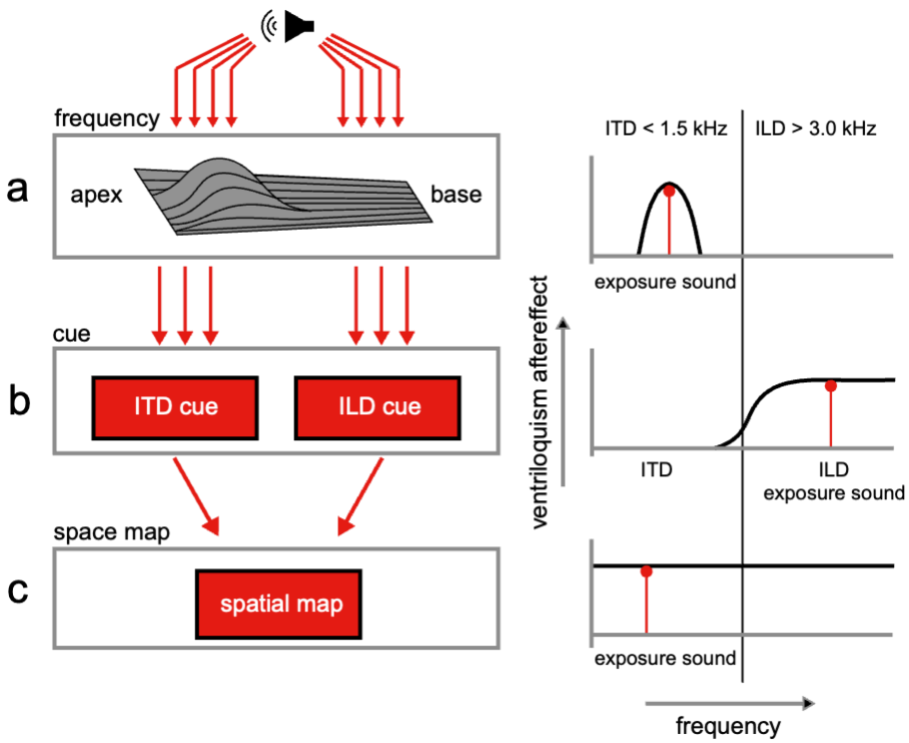

Figure 1. Ventriloquism aftereffect models. ***a)*** *The influence of the light on sound localisation takes place at a tonotopic stage (left column). The ventriloquism aftereffect is then only found for frequencies within a critical band (right column, black curve) around the exposure frequency (right column, red vertical line with dot on the top).* ***b)*** *The light influences sound localisation when the ITD or ILD cues have been extracted (left column). The ventriloquism aftereffect will be restricted to frequencies belonging to that cue (right column, the black curve for ILD cues, given the frequency of the exposure sound, in red). The thin vertical line represents the border between the ITD and ILD domains (around 2 kHz).* ***c)*** *Generalization across the entire frequency domain occurs if the light influences sound localisation at the level of a spatial map (left column). The aftereffect will generalize across all frequencies (left column, black line).*

Materials and Methods

Participants

Twelve human participants provided their informed consent and performed the experiments. All participants had normal or corrected-to-normal vision and normal hearing (verified by means of a sound localisation experiment including low-pass, high-pass and Gaussian white noise sounds in the frontal hemifield, and a standard audiogram). Three participants helped in the execution of the study; the other

participants were kept naive about the purpose of the study. The experimental protocol was approved by local institutional ethical committee of the Faculty of Social Sciences at the Radboud University (ECSW 2016-2208-41), and all applied procedures were in line with the relevant guidelines and regulations.

Apparatus

During the experiment, the participant sat in a chair in the centre of a completely dark, sound-attenuated room. The room had an ambient background noise level below 30 dBA. The chair was positioned at the centre of a spherical frame (radius 1.5 m), on which 125 small broad-range loudspeakers (SC5.9; Visaton GmbH, Haan, Germany) were mounted. Green LEDs (wavelength 565 nm; Kingsbright Electronic Co., LTD., Taiwan; luminance 1.4 cd/m^2) were mounted at the centre of each speaker. For a more thorough description of the room, see [24]. Head movements were recorded with the magnetic search-coil technique[25]. To this end, the participant wore a lightweight spectacle frame with a small coil attached to their nose bridge. The horizontal and vertical head-coil signals were amplified and demodulated (EM7; Remmel Labs, Katy, TX, USA), low-pass-filtered at 150 Hz (custom built, fourth-order Butterworth), digitized (RA16GA and RA16; Tucker-Davis Technology, Alachua, FL, USA) and stored on hard disk at 6 kHz/channel. A custom-written MATLAB program, running on a PC (HP EliteDesk, California, United States) controlled data recording and storage, stimulus generation, and online visualization of the recorded data.

Stimuli

Sounds were pre-generated as white noise. Seven narrowband sounds were created by band-pass filtering to have a bandwidth of 2/3 octaves around centre frequencies {500, 793, 1260, 2000, 3175, 5040, 8000} Hz. A broadband sound was generated by band-pass filtering between 0.5 and 20 kHz. All sounds had a duration of 75 ms, with 5-ms sine-squared onset, and cosine-squared offset ramps, and were presented at an A-weighted level of L_A = 55 dB.

Calibration

To determine the off-line calibration that maps the raw coil signals (in mV) onto known target locations (in deg), participants pointed their head towards 24 LED locations in the frontal hemifield (separated by approximately 30 deg in both azimuth and elevation). The pointing was done via a red LED that was attached to the spectacle frame, at a fixed distance of 40 cm in front of the eyes. This setup ensured the position of the eyes was aligned with the head movements. A three-layer neural network (implemented in MATLAB) was trained to map the raw initial and final head position signals onto the (known) LED azimuth and elevation angles, with an overall accuracy of 1.0 deg or better. The weights of the neural network were subsequently used to map all head-movement voltages of the localisation experiments to degrees.

Paradigm

Participants were instructed to localise sounds. Each participant performed three sessions, each on a separate day. Each session consisted of three phases: pre-exposure, exposure, and post-exposure. During the pre- and post-exposure phases we presented eight sounds. During the exposure phase, one sound was presented in combination with an offset visual stimulus. This sound was either a 793 Hz, a 5040 Hz, or a broadband sound, using a different sound for each session. These stimuli were chosen to target specific localisation cues; a low-frequency narrowband sound to target ITDs, a high-frequency narrowband sound to target ILDs, and a broadband sound to target both cues. In the pre-exposure phase, we measured sound localisation performance, in the exposure phase we determined the ventriloquism effect, and in the post-exposure phase we obtained the ventriloquism aftereffect.

The design of the pre- and post-exposure phases were the same. Target sounds were presented at eight locations in the horizontal plane (-35 to +35 deg, in 10 deg steps). Each stimulus-location combination was presented four times in pseudo-random order (8 sounds x 8 locations x 4 repeats = 256 trials). During the exposure phase, one of three sounds was presented at the same eight locations (-35 to +35 deg, in steps of 10 deg), while simultaneously a LED was presented ten degrees to the right (-25 to +45 deg, in steps of 10 deg). Each stimulus-location combination was repeated 56 times, resulting in 448 trials (56 repeats x 8 locations). In each trial, participants first aligned the head-fixed laser with a central fixation light (Fig. 2). A fixation light was presented at the centre speaker (0 deg azimuth and 0 deg elevation) at the start of each trial, to ensure participants had a similar starting position over trials. The fixation light was extinguished with a random timing between 300-800 ms. After the fixation light there was a gap of 200 ms before the target stimulus was presented. Participants were asked to align the head-fixed laser pointer as quickly and as accurately as possible with the sound source's origin (neglecting the light). One session took approximately 60 minutes, which includes the calibration and short breaks in between the blocks.

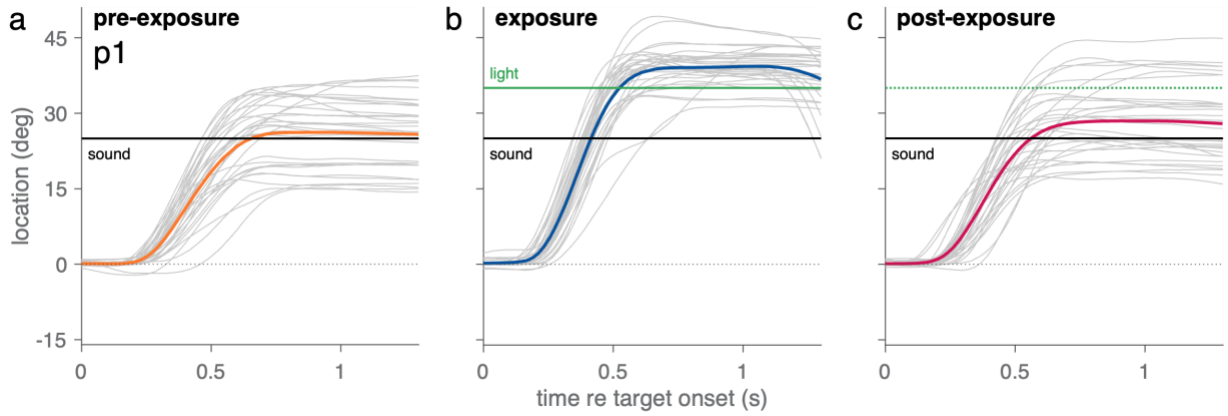

Figure 2. Head-orientation responses across experimental phases. *Data shown are from a single participant (P1) during the three phases of one session (exposure sound: 5040 Hz). a) Pre-exposure phase. Head orientation traces (grey) in response to eight different test sounds presented at 25° (black line). Final*

head positions cluster around the sound location. The average response trace (orange) shows accurate localisation at the end of the rapid head orienting movement. b) Exposure phase. Head orientation traces to repeated presentations of a single narrowband sound (centre frequency: 5040 Hz) at 25°, paired with a visual distractor at 35° (green line). The average trace (blue) overshoots the sound location, ending near the light at 39°, indicating a ventriloquism effect. c) Post-exposure phase. Head orientation traces in response to the eight test sounds at 25°, now presented without the light. The average trace (pink) is biased toward the former visual distractor location, indicating a ventriloquism aftereffect.

Data Analysis

Modelling approach

Participants were instructed to localise band-limited noise bursts. In the pre-exposure phase, these sounds were presented in isolation, in complete darkness, and without any visual stimulus. This setup allowed us to assess baseline sound-localisation performance. Auditory responses (R_s) were well approximated by a linear function passing through the origin, proportional to the true target location (T) (see Fig. 3, blue). We therefore modelled responses as:

$$R_S = g_S T \qquad \text{Eq. 1}$$

Here, g_S is the target-response or sound-localisation (S) gain (the slope of the target-response function). The gain is unitless and reflects how accurately perceived location tracks true location, with 1 reflecting perfect accuracy and 0 reflecting an absence of a relationship. With eight sound frequencies and twelve participants, this results in 96 gain estimates. Rather than estimating a separate gain for each frequency and participant, we expressed each gain g_S as a linear combination of fixed and random effects:

$$g_S = g_0 + \vec{g}_f \vec{x}_f + \vec{g}_p \vec{x}_p + \vec{g}_{f\times p} \vec{x}_{f\times p} \qquad \text{Eq. 2}$$

Here, g_o is the grand average gain, g_f, g_p, and $g_{f\times p}$ are the effects of frequency, participant, and their interaction, x_f, x_p, and $x_{f\times p}$ are the corresponding design vectors (e.g., indicator variables or contrast codes). These components reflect deviations from the grand average g_o due to frequency-specific and participant-specific effects, or their interaction. To illustrate the model, Fig. 3 shows data from example participant P2 for two sound frequencies: 793 Hz and 2000 Hz. The participant localised the 793-Hz sound with an overshoot (g_S = 1.34; Fig. 3a, yellow). This estimate decomposed as: an average gain g_o = 1.29, a frequency effect g_f = +0.07, a participant effect g_p = –0.12 and an interaction effect $g_{f\times p}$ = +0.1. For the 2000-Hz sound, the same participant showed accurate localisation with a slight undershoot (g_S = 0.93; Fig. 3b, yellow). This was decomposed into: g_o = 1.29 (same), g_f = -0.17, g_p = –0.12 (same), and $g_{f\times p}$ = -0.08. In both cases, the best-fit line (yellow) closely matched the observed data (yellow dots).

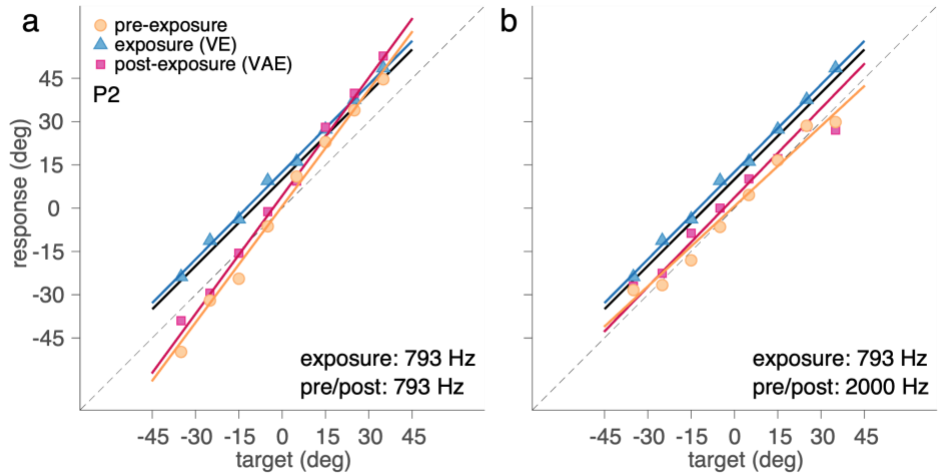

Figure 3. Example data and model fits. *Target–response relationships for two sounds during the pre-exposure, exposure, and post-exposure phases. Panels show data from one participant (P2) for test sounds with a centre frequency at* ***(a)*** *793 Hz and* ***(b)*** *2000 Hz. In both cases, the exposure sound was a 793-Hz sound. Individual responses are shown as orange dots (pre-exposure), blue triangles (exposure), and pink squares (post-exposure); lines represent the corresponding model fits. The solid black bold diagonal line marks the location of the visual stimulus presented during the exposure phase (10° offset from the sound). The dashed black diagonal line indicates perfect localisation of the sound target.*

During the exposure phase (Fig. 3, blue), sound localisation was systematically influenced by a visual stimulus (*V*) displayed 10 deg to the right of the auditory target (*T*). To quantify this ventriloquism effect, we modelled the response (R_{VE}) as a linear function of both the auditory target location and the audiovisual disparity (*D*):

$$R_{VE} = g_{VE}T + b_{VE}D \qquad \text{Eq. 3}$$

Here, g_{VE} is the ventriloquism-effect gain (slope) in the presence of a visual stimulus and b_{VE} is the ventriloquism-effect bias, a unitless parameter that reflects the proportion of the audiovisual disparity, *D*, that is incorporated into the participant's response, with 1 reflecting a full bias towards the visual stimulus and 0 reflecting an absence of a visual bias. Importantly, this disparity *D* is not simply the physical 10° offset between the sound and visual stimulus, but rather the difference between the visual location *V* and the auditory response location:

$$D = V - R_S = T + 10 - g_S T \qquad \text{Eq. 4}$$

This definition of *D* centres the bias on the disparity between the visual stimulus and where the auditory target would have been localised in the absence of visual input (Eq. 1 and 2). With three exposure

sounds and twelve participants, this results in 36 gain and 36 bias estimates. We expressed each gain and bias parameter as a linear combination of exposure sound (*e*), participant (*p*), and interaction effects, analogous to Eq. 2.

The slope and offset of the target-response line (as shown in Fig. 3, blue line) are the target-response gain and bias, and can be derived from g_{VE}, b_{VE}, and g_S from Eqs. 3 and 4 as follows:

$$\begin{aligned} R_{VE} &= g_{VE}T + b_{VE}T + 10b_{VE} - b_{VE}g_S T \\ &= (g_{VE} + b_{VE} - b_{VE}g_S)T + 10b_{VE} \\ &\equiv G_{VE}T + B_{VE} \end{aligned} \qquad \text{Eq. 5}$$

The target-response gain G_{VE} (dimensionless) and bias B_{VE} (in deg) during the exposure phase are then given by:

$$\begin{aligned} G_{VE} &= g_{VE} + b_{VE} - b_{VE}g_s \\ B_{VE} &= 10b_{VE} \end{aligned} \qquad \text{Eq. 6}$$

In this way, if b_{VE} is 0, G_{VE} reduces to g_{VE} and B_{VE} to 0 deg. If also $g_{VE} = g_s$, sound localisation would not be affected by the visual stimulus, $R_{VE} = g_S T = R_s$. If b_{VE}=1, G_{VE} reduces to $g_{VE} - g_s + 1$, and B_{VE} to 10 deg. If also $g_{VE} = g_s$, sound localisation is completely dominated by the visual stimulus, $R_{VE} = T + 10 = V$. This analysis enables us to assess whether the presence of a simultaneous visual stimulus affects not only bias (as in the classical ventriloquism effect) but also the localisation slope, which may reflect changes in under- or overshooting behaviour. To illustrate, Fig. 3 (blue lines and triangles; note that panels a and b show the same exposure data) shows responses from participant P2 for the 793-Hz exposure sound. This participant was heavily influenced by the visual stimulus with a target-response gain near 1 (G_{VE} = 1.0) and a bias near 10 deg (B_{VE} = 12 deg). This indicates that the participant responded to the visual distractor, seemingly fully ignoring the auditory target.

To quantify the ventriloquism aftereffect, we modelled the response (R_{VAE}) in the post-exposure phase as a linear function of the auditory target location and the remembered visual-auditory disparity (D) from the preceding exposure phase:

$$R_{VAE} = g_S T + b_{VAE} D \qquad \text{Eq. 7}$$

Here, g_S is the sound-localisation gain, shared across the pre- and post-exposure phase for all three sessions. The aftereffect bias b_{VAE} is a unitless proportion indicating the extent to which the response remains biased toward the location of the previously presented visual distractor, despite the absence of visual input during the post-exposure phase. A value of 0 indicates no aftereffect, while a value of 1 would indicate a complete shift equivalent to the prior visual offset. The gain and bias are estimated following the form of Eq. 2: g_S for each test frequency (*f*) and participant (*p*), and b_{VAE} for each test frequency (*f*),

exposure sound (*e*), and participant (*p*). With eight test frequencies, three exposure sounds, and twelve participants, this results in 96 gain estimates (g_S), and 288 bias estimates (b_{VAE}).

Importantly, g_S was estimated using both pre- and post-exposure data, and we did not model a separate ventriloquism-aftereffect gain (as for the ventriloquism effect). We assumed that the sound-localisation gain would not be affected, as no visual stimulus was presented in both the pre-exposure (sound-localisation) phase and post-exposure (aftereffect) phase. A prior analysis indicated that localisation gain did not significantly differ between these phases or across sessions, justifying this pooling strategy and allowing for more stable parameter estimates. To illustrate the model, Fig. 3 (pink lines and squares) shows post-exposure data from participant P2. For the 793-Hz test sound (Fig. 3a), the response was biased toward the location of the prior visual stimulus, with B_{VAE} = 4.3 deg. For the 2000-Hz sound (Fig. 3b), the aftereffect was lower (B_{VAE} = 2.2 deg) than that of the 793-Hz sound (Fig. 3a).

The target-response gain G_{VAE} (dimensionless) and bias B_{VAE} (in deg) during the exposure phase can be derived from Eq. 7 as follows:

$$\begin{aligned} R_{VAE} &= g_S T + b_{VAE} T + 10 b_{VAE} - b_{VAE} g_S T \\ &= (g_S(1 - b_{VAE}) + b_{VAE})T + 10 b_{VAE} \\ &\equiv G_{VAE} T + B_{VAE} \end{aligned} \qquad \text{Eq. 8}$$

which yields:

$$\begin{aligned} G_{VAE} &= g_S(1 - b_{VAE}) + b_{VAE} \\ B_{VAE} &= 10 b_{VAE} \end{aligned} \qquad \text{Eq. 9}$$

In this way, if b_{VAE} is 0, g_{VAE} reduces to g_S and B_{VAE} to 0 deg. This would imply there is no ventriloquism aftereffect, $R_{VAE} = g_S T = R_S$. If b_{VAE} = 1, G_{VAE} reduces to 1, and B_{VAE} to 10 deg. This would imply that the ventriloquism aftereffect, $R_{VAE} = T + 10 = V$.

Bayesian Statistical Analysis

We used Bayesian inference to estimate model parameters from the observed data. Bayesian methods were chosen because they provide full posterior distributions for each parameter, offering both point estimates (e.g., means or medians) and credible intervals that quantify the uncertainty associated with these estimates. This approach allows for flexible implementation of complex hierarchical models, enabling simultaneous estimation at multiple levels.

All continuous variables were z-scored prior to analysis to facilitate parameter estimation. We applied standard normal priors (mean = 0, SD = 1) to the model parameters. These priors are weakly informative and appropriate for standardized data. To help the model converge, we based the prior mean for the ventriloquism bias on the mean effect observed in prior analyses. To account for individual variability and improve generalizability, all factors in the model — including test frequency, exposure

frequency, and participant — were estimated using a hierarchical structure, allowing for partial pooling across levels of each factor. This approach reduces overfitting and provides more stable parameter estimates, particularly in conditions with sparse data. To aid interpretation, posterior estimates from the standardized model were back-transformed to the original scale using the means and standard deviations of the raw data, restoring units that are meaningful in the context of the observed behaviour.

Model fitting was performed via Markov Chain Monte Carlo sampling, in MATLAB (Mathworks, version R2021b), using the 'matjags' interface[26] for JAGS[27]. Convergence was assessed using standard diagnostics, including the Gelman–Rubin statistic (all Rhat < 1.1)[28] and effective sample size. To evaluate model fit, we performed posterior predictive checks, comparing model-generated data to observed patterns.

Estimation statistics

We summarized the results of the Bayesian analysis using both point estimates (posterior means) and interval estimates (95% highest density intervals, HDI). Point estimates provide the most probable value of the parameters given the data, while the interval estimates give a range of plausible values. The 95% HDI is the smallest interval which contains 95% of the probability density, with points outside of the range having a lower probability density than those within it. This interval represents the range of values that most likely contains the true value of a parameter, given the current data and statistical model.

Results

To examine how the ventriloquism aftereffect generalizes across sound frequencies, participants localised sounds at various horizontal positions using head movements. Each participant completed three experimental sessions, each consisting of a pre-exposure, exposure, and post-exposure phase. During the exposure phase, one of three sounds—a low-frequency, high-frequency, or broadband sound—was paired with a visual stimulus located 10° to the right of the auditory target. Each of these sounds was tested in a separate session. In the pre- and post-exposure phases, participants localised eight sounds—seven narrowband and one broadband—without any visual stimulus. This design allowed us to assess baseline sound-localisation performance and determine the presence and generalization of the ventriloquism aftereffect. Specifically, we tested whether the aftereffect was limited to the sound presented during exposure, generalized within cue types (low-frequency ITD vs. high-frequency ILD), or extended across the entire frequency spectrum.

We begin by presenting results on the ventriloquism effect—sound localisation in the presence of a simultaneous visual distractor—followed by the ventriloquism aftereffect, which reflects localisation shifts following prior exposure to audiovisual disparity. For both effects, we also report baseline sound-only localisation behaviour to characterize cue reliability.

The ventriloquism effect

To assess the effect of a simultaneous visual stimulus on sound localisation, we analysed response gains and visual biases for the three sounds used during the exposure phases (793 Hz narrowband, 5040 Hz narrowband, and broadband). Figure 4a shows the target-response gains in the pre-exposure phase (g_s; orange circles) and during the exposure phase (G_{VE}; purple squares). In the pre-exposure phase (sound only), participants localised broadband sounds with high accuracy, yielding an average gain of 1.16 [1.14, 1.17]. In contrast, they exhibited overshooting for the narrowband sounds, with gains of around 1.3 [1.29, 1.31]. During the exposure phase (sound plus light), target-response gains were more accurate, being on average 1.03 [1.03, 1.04]. This high accuracy (gain close to 1) suggests that the presence of a visual stimulus improved localisation accuracy for narrowband sounds.

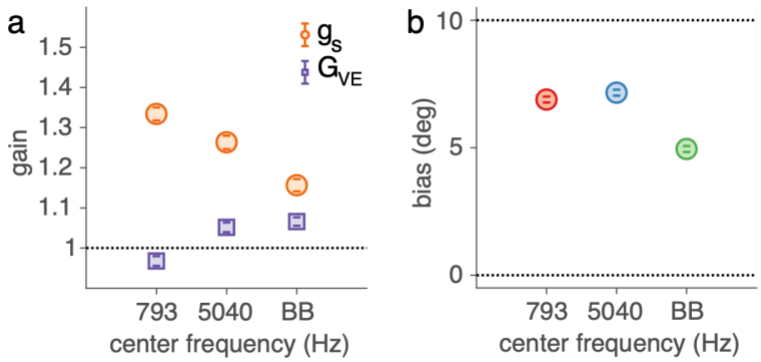

Figure 4. Ventriloquism effect. ***a)*** *The sound-localisation response gains during the pre-exposure phase (g_s, in orange) and the exposure phase (G_{VE}, in purple).* ***b)*** *The bias (B_{VE}) in deg for the three exposure sounds during the exposure phase. The mean and 95%-HDI of the posterior distribution on these parameter estimates are depicted as coloured circles and vertical error bars.*

We also observed a robust bias (B_{VE}) toward the visual distractor (Fig. 4b) in the exposure phase. The average bias across all sounds was 6.3 [6.3, 6.4] deg. This bias was stronger for narrowband sounds (7 [6.9, 7.1] deg) than for broadband sounds (5 [4.8, 5.1] deg). These results confirm a clear ventriloquism effect: a simultaneous light biased sound localisation, especially for narrowband stimuli.

The ventriloquism aftereffect

Next, we analyzed sound-localization gains in the pre- and post-exposure phases to characterize how localization responses varied with sound frequency before and after visual exposure. Specifically, we estimated the pre-exposure gain (g_s; orange circles) and the post-exposure gain (G_{VAE}; purple squares) for the eight test sounds (Fig. 5a). Both g_S and G_{VAE} showed a strong dependence on sound frequency. During the post-exposure phase, broadband sounds were localized with high accuracy, yielding a gain of 1.17

[95% HDI: 1.15, 1.18]. Narrowband sounds showed a characteristic V-shaped pattern, with the highest gains for the lowest and highest center frequencies, peaking at 1.46 [1.42, 1.47] for the 500 Hz sound, consistent with overshooting, and the lowest gain for the 2000 Hz sound (1.12 [1.11, 1.14]). Importantly, the gains in the post-exposure phase (G_{VAE}) systematically differed from the pre-exposure gains (g_S). As explained in the Methods, this difference reflects the influence of a bias component (Eq. 8). In other words, the observed changes in gain during the pre- and post-exposure phase indirectly reflect the ventriloquism aftereffect.

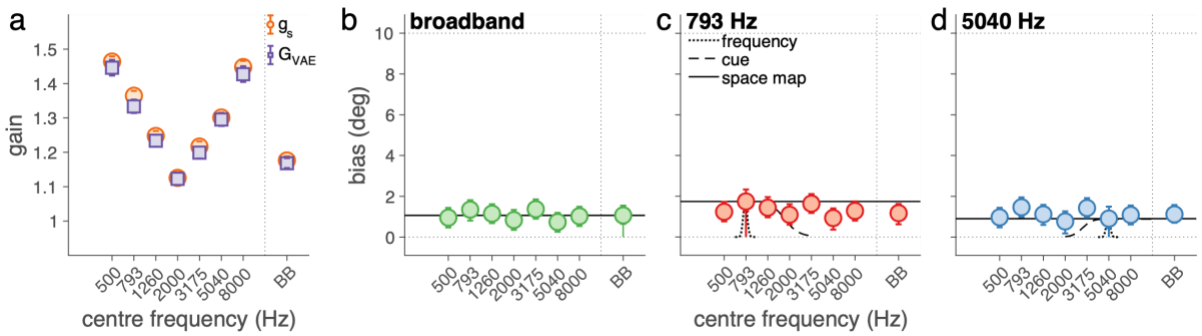

Figure 5. Ventriloquism aftereffect. ***a)*** *The sound localisation gains, g_s, pooled over pre- and post-exposure data for the eight test sounds, and the derived target-response gains, G_{VAE}.* ***b-d)*** *The ventriloquism aftereffect bias, B_{VAE}, for the* ***b)*** *broadband (BB),* ***c)*** *low-frequency (793 Hz), and* ***d)*** *high-frequency (5040 Hz) exposure sound as a function of test sound frequency. The mean and 95%-HDI of the posterior distribution on these parameter estimates are depicted as coloured circles and vertical error bars.*

We analysed this aftereffect more directly by quantifying the bias term B_{VAE}, which reflects the difference in perceived sound location between the pre- and post-exposure phases (Figs. 5b-d). The biases were relatively consistent, between 0.7 and 1.7 deg, suggesting that the aftereffect generalized beyond the specific exposure frequency to some extent. The magnitude of the aftereffect was similar across exposure sounds: 1.2 [1.0, 1.3] deg. Crucially, for the narrowband exposure sounds (Figs. 5b, c), a considerable aftereffect was present even for test sounds with a centre frequency far from the exposure centre frequency (e.g., the bias for the 8000-Hz test sound after 793 Hz exposure was 1.3 [0.8, 1.7] deg, Fig. 5c). This suggests that exposure to a low-frequency sound did not selectively bias low-frequency test sounds more than others, and similarly for high-frequency exposure. Taken together, these results show that the ventriloquism aftereffect, while small, is robust and broadly generalizable across the tested frequency range.

Discussion

Overview

This study investigated how the ventriloquism effect and its aftereffect depend on the spectral properties of sounds, to test whether these audiovisual interactions arise within frequency-specific auditory pathways or from a shared, frequency-independent spatial map. Participants localised sounds using head movements across three experimental phases: a baseline (pre-exposure), an audiovisual exposure (ventriloquism), and a post-exposure (aftereffect) phase. Each exposure phase involved one of three sounds—low-frequency, high-frequency, or broadband—paired with a consistent visual offset, while the aftereffect was probed using eight different sounds spanning a wide spectral range.

We found that sound localisation with narrowband noise was inaccurate and frequency-dependent, with overshoots particularly at low and high frequencies. Broadband sounds were localised accurately, presumably due to the presence of more reliable spatial cues. During the exposure phase, the ventriloquism effect varied across the three exposure sounds: broadband sounds showed the smallest bias, consistent with their higher spatial reliability. Moreover, the ventriloquism effect impacted not only bias but also the target-response gain, indicating that the presence of a visual stimulus alters both perceived direction and the slope of the auditory spatial response. The aftereffect was evident as a lasting bias in sound localisation, even in the absence of visual input. Importantly, the aftereffect generalized broadly across frequencies, regardless of whether the exposure sound was low-frequency, high-frequency, or broadband. That is, adaptation to an audiovisual discrepancy in one frequency band influenced localisation responses to sounds across the spectrum.

Inaccuracy of narrowband sound localisation

A key feature of our study is the precise quantification of localisation accuracy for narrowband sounds. Consistent with earlier tone-localisation studies[29–33], our data revealed large, frequency-dependent deviations between the perceived and actual locations of narrowband stimuli (Figs. 4a, 5a, orange). In contrast, broadband sounds were localised with high accuracy, showing only a slight overshoot. This discrepancy likely reflects differences in the reliability of spatial cues available for each sound type. Narrowband sounds primarily provide information through either interaural time differences (ITDs, e.g., 793 Hz) or interaural level differences (ILDs, e.g., 5040 Hz), but not both. While these cues support horizontal localisation, the resulting gains deviated substantially from unity—by approximately 29%—highlighting a consistent overshoot. Additionally, narrowband sounds offer poor spectral content, rendering spectral elevation cues unreliable and making it impossible to resolve front-back or elevation ambiguities, often referred to as the 'cone of confusion'[34]. In contrast, broadband sounds provide rich spatial information, including ITDs, ILDs, and spectral shape cues, enabling the auditory system to form a more precise and reliable spatial estimate. Thus, the lower localisation accuracy for narrowband sounds is best understood because of reduced cue reliability and ambiguity in spatial encoding.

Mechanisms in the ventriloquism effect

All three exposure sounds elicited a pronounced ventriloquism effect, traditionally defined as a spatial bias in auditory perception toward a simultaneously presented visual stimulus. This effect was strongest for the two narrowband sounds and slightly weaker for the broadband sound (Fig. 4b). This pattern aligns with the principles of Bayesian sensory integration, where the brain combines sensory inputs based on their relative uncertainties, weighting more reliable inputs more heavily[2,35–37]. Since broadband sounds offer rich spatial cues and are localised more accurately (as discussed in the previous section), they are treated as more reliable by the brain and are therefore less influenced by the visual distractor. Narrowband sounds, in contrast, provide ambiguous and less reliable spatial information—especially due to their frequency-specific overshoots and unresolved cone-of-confusion ambiguities. As a result, auditory-visual integration is more heavily dominated by the visual modality for these stimuli, producing a larger visual bias. Interestingly, the ventriloquism effect for narrowband sounds was not limited to a shift (bias) in perceived location—it also included a change in gain (Fig. 4a). Due to the substantial overshoots in narrowband sound localisation, the perceived audiovisual disparity was not constant across the spatial range. For example, a 10° visual offset could appear larger or smaller depending on how the auditory target was mislocalised. Consequently, the visual influence effectively varied with target location, leading to changes in both response gain and bias during the exposure phase. This dual modulation illustrates that the ventriloquism effect, particularly for unreliable auditory signals, is more complex than a fixed spatial shift.

Mechanisms in the ventriloquism aftereffect

We next examined the ventriloquism aftereffect across different combinations of exposure and test sounds. On average, participants exhibited a moderate aftereffect, with post-exposure sound-localisation responses biased by approximately 12% of the perceived audiovisual disparity (Figs. 5b-d). This was independent of the exposure sound. The aftereffect showed broad generalization across all tested sound frequencies, suggesting that the aftereffect generalized across the auditory spectrum. The observed pattern of broad generalization contrasts with predictions from computational models by Magosso et al. [22,23] and earlier studies [4–6,9], which suggested that at moderate sound levels (~55 dB), frequency-specific adaptation should dominate. In our study, however, we observed generalization across the frequency spectrum, indicating that sound level alone may not fully determine the extent of generalization. Future studies should more systematically vary sound intensity to assess whether generalization with perceptual reliability.

Conclusion

A broad generalization of the ventriloquism aftereffect across sound frequencies strongly supports the hypothesis that the aftereffect reflects adaptation within a multisensory spatial

representation, where auditory and visual signals are integrated into a shared topographic map. The reduced susceptibility of broadband sounds to the ventriloquism effect suggests a contribution of priors on sensory uncertainty. Taken together, these findings point to a role for both acoustic and non-acoustic factors in modulating the aftereffect. To conclude, the ventriloquism aftereffect reflects adaptive changes at a higher-level, modality-independent spatial map.

Author contributions

A.J.v.O.: Funding acquisition, Resources, Supervision, and Writing - review & editing.

M.M.v.W.: Conceptualization, Data curation, Formal analysis, Funding acquisition, Methodology, Resources, Software, Supervision, Visualization, and Writing - review & editing.

N.C.H.: Formal analysis, Investigation, Project administration, Software, Validation, Visualization, and Writing - review & editing.

R.E.: Formal analysis, Funding acquisition, Investigation, Project administration, Visualization, Writing - original draft, and Writing - review & editing.

Acknowledgements

We thank Günter Windau, Ruurd Lof, and Stijn Martens for their valuable technical assistance. We are also grateful to the volunteers for their participation in these experiments. Lastly, we thank Sem van Lankveld and Joep Ritzen for their assistance in the research project.

Funding

A.J. van Opstal was supported by European Union Horizon-2020 ERC Advanced Grant 2016 (ORIENT, nr. 693400); Rachel Ege was supported by NWO-MaGW Talent, grant nr. 406-11-174.

Data availability

The data are openly available in the Data Sharing Collection of the Donders Repository at https://doi.org/10.34973/gbq9-yd62

Additional Information

Competing Interests: The authors declare no competing interests.

References

1. Middlebrooks, J. C. & Green, D. M. Sound localization by human listeners. *Annual review of psychology* **42**, 135–159 (1991).
2. Opstal, A. J. *The Auditory System and Human Sound-Localization Behavior*". (Academic Press, Elsevier, Amsterdam, The Netherlands, 2016).
3. Radeau, M. & Bertelson, P. The After-Effects of Ventriloquism. *Quarterly Journal of Experimental Psychology* **26**, 63–71 (1974).
4. Recanzone, G. H. Rapidly induced auditory plasticity: The ventriloquism aftereffect. *Proc. Natl. Acad. Sci. U.S.A.* **95**, 869–875 (1998).
5. Lewald, J. Rapid Adaptation to Auditory-Visual Spatial Disparity. *Learn. Mem.* **9**, 268–278 (2002).
6. Frissen, I., Vroomen, J., De Gelder, B. & Bertelson, P. The aftereffects of ventriloquism: Are they sound-frequency specific? *Acta Psychologica* **113**, 315–327 (2003).
7. Canon, L. K. Intermodality inconsistency of input and directed attention as determinants of the nature of adaptation. *Journal of Experimental Psychology* **84**, 141–147 (1970).
8. Jack, C. E. & Thurlow, W. R. Effects of degree of visual association and angle of displacement on the ventriloquism effect. *Percept. Mot. Skills* **37**, 967–979 (1973).
9. Frissen, I., Vroomen, J., Gelder, B. & Bertelson, P. The aftereffects of ventriloquism: generalization across sound frequencies. *Acta Psychol* **118**, 93–100 (2005).
10. Frissen, I., Vroomen, J. & De Gelder, B. The Aftereffects of Ventriloquism: The Time Course of the Visual Recalibration of Auditory Localization. *Seeing and Perceiving* **25**, 1–14 (2012).
11. Woods, T. M. & Recanzone, G. H. Visually Induced Plasticity of Auditory Spatial Perception in Macaques. *Current Biology* **14**, 1559–1564 (2004).

12. Kopco, N., Lin, I.-F., Shinn-Cunningham, B. G. & Groh, J. M. Reference frame of the ventriloquism aftereffect. *J. Neurosci* **29**, 13809–13814 (2009).

13. Bruns, P. & Röder, B. Sensory recalibration integrates information from the immediate and the cumulative past. *Sci. Rep* **5**, 12739 (2015).

14. Bruns, P. & Röder, B. Spatial and frequency specificity of the ventriloquism aftereffect revisited. *Psychological Research* **83**, 1400–1415 (2019).

15. Bosen, A. K., Fleming, J. T., Allen, P. D., O'Neill, W. E. & Paige, G. D. Accumulation and decay of visual capture and the ventriloquism aftereffect caused by brief audio-visual disparities. *Exp. Brain Res* **235**, 585–595 (2017).

16. Bosen, A. K., Fleming, J. T., Allen, P. D., O'Neill, W. E. & Paige, G. D. Multiple time scales of the ventriloquism aftereffect. *PLoS One* **13**, 0200930 (2018).

17. Zierul, B., Röder, B., Tempelmann, C., Bruns, P. & Noesselt, T. The role of auditory cortex in the spatial ventriloquism aftereffect. *Neuroimage* **162**, 257–268 (2017).

18. Berger, C. C. & Ehrsson, H. H. Mental Imagery Induces Cross-Modal Sensory Plasticity and Changes Future Auditory Perception. *Psychol Sci* **29**, 926–935 (2018).

19. Schooneveldt, G. P. & Moore, B. C. J. Comulation masking release (CMR) as a function of masker bandwidth, modulator bandwidth and signal duration. *J Acoust Soc Am* **85**, 273–281 (1989).

20. Moore, B. C. J. *An Introduction to the Psychology of Hearing*". (Brill Publishers, Leiden, Netherlands, 2013).

21. Corneil, B. D., Wanrooij, M. M., Munoz, D. P. & Opstal, A. J. Auditory-visual interactions subserving goal-directed saccades in a complex scene. *J. Neurophysiol* **88**, 438–454 (2002).

22. Magosso, E., Cuppini, C. & Ursino, M. A Neural Network Model of Ventriloquism Effect and Aftereffect. *PLoS ONE* **7**, e42503 (2012).

23. Magosso, E., Cona, F. & Ursino, M. A Neural Network Model Can Explain Ventriloquism Aftereffect and Its Generalization across Sound Frequencies. *BioMed Research International* **2013**, 1–17 (2013).

24. Van Bentum, G. C., Van Opstal, A. J., Van Aartrijk, C. M. M. & Van Wanrooij, M. M. Level-weighted averaging in elevation to synchronous amplitude-modulated sounds. *The Journal of the Acoustical Society of America* **142**, 3094–3103 (2017).

25. Robinson, D. A. A method of measuring eye movemnent using a scieral search coil in a magnetic field. *IEEE Transactions on bio-medical electronics*, *10*(4), 137-145 (1963).

26. Steyvers, M. MATJAGS 13 A Matlab interface for JAGS. Available at http://psiexp.ss.uci.edu/research/programs_data/jags/ (2011).

27. Plummer, M. JAGS: A program for analysis of Bayesian graphical models using Gibbs sampling. in *Proceedings of the 3rd International Workshop on Distributed Statistical Computing (DSC 2003* (Vienna, Austria, 2003).

28. Gelman, A. & Rubin, D. B. Inference from iterative simulation. *Statistical Science* vol. 7 457–511 Preprint at (1992).

29. Musicant, A. D. & Butler, R. A. The influence of pinnae-based spectral cues on sound localization. *The Journal of the Acoustical Society of America* **75**, 1195–1200 (1984).

30. Middlebrooks, J. C. Narrow-band sound localization related to external ear acoustics. *The Journal of the Acoustical Society of America*, *92*(5), 2607-2624. (1992).

31. Goossens, H. H. L. M. & Opstal, A. J. Influence of head position on the spatial representation of acoustic targets. *Journal of neurophysiology* **81**, 2720–2736 (1999).

32. Van Grootel, T. J., Van Wanrooij, M. M. & Van Opstal, A. J. Influence of Static Eye and Head Position on Tone-Evoked Gaze Shifts. *J. Neurosci.* **31**, 17496–17504 (2011).

33. Hofman, P. M., Riswick, J. G. & Opstal, A. J. Relearning sound localization with new ears. *Nature neuroscience* **1**, 417–421 (1998).

34. Blauert, J. *Spatial Hearing: The Psychophysics of Human Sound Localization*. (MIT press, 1997).

35. Alais, D. & Burr, D. The Ventriloquist Effect Results from Near-Optimal Bimodal Integration. *Current Biology* **14**, 257–262 (2004).

36. Ege, R., Opstal, A. J. V. & Van Wanrooij, M. M. Accuracy-Precision Trade-off in Human Sound Localisation. *Sci Rep* **8**, 16399 (2018).

37. Ernst, M. O. & Banks, M. S. Humans integrate visual and haptic information in a statistically optimal fashion. *Nature* **415**, 429–433 (2002).

38. Kayser, C., Park, H. & Heuer, H. Cumulative multisensory discrepancies shape the ventriloquism aftereffect but not the ventriloquism bias. *PLoS ONE* **18**, e0290461 (2023).

39. Park, H. & Kayser, C. The context of experienced sensory discrepancies shapes multisensory integration and recalibration differently. *Cognition* **225**, 105092 (2022).

40. Kayser, C. & Heuer, H. Perceived Multisensory Common Cause Relations Shape the Ventriloquism Effect but Only Marginally the Trial-Wise Aftereffect. *Eur J of Neuroscience* **61**, e70015 (2025).